LA-UR- 11-05191

Approved for public release; distribution is unlimited.

Title: Experimental Demonstration of Terahertz Metamaterial Absorbers with a Broad and Flat High Absorption Band

Author(s): Li Huang, Dibakar Roy Chowdhury, Suchitra Ramani, Matthew T. Reiten, Sheng-Nian Luo, Antoinette J. Taylor, Hou-Tong Chen

Intended for: Optics Letters

Los Alamos
NATIONAL LABORATORY
EST. 1943

Experimental demonstration of terahertz metamaterial absorbers with a broad and flat high absorption band

Li Huang,[1,2,*] Dibakar Roy Chowdhury,[2] Suchitra Ramani,[2] Matthew T. Reiten,[2] Sheng-Nian Luo,[3] Antoinette J. Taylor,[2] and Hou-Tong Chen[2,*]

[1] *Physics Department, Harbin Institute of Technology, Harbin, Heilongjiang 150001, China*
[2] *Los Alamos National Laboratory, MPA-CINT, MS K771, Los Alamos, New Mexico 87545, USA*
[3] *Los Alamos National Laboratory, P-25, MS H846, Los Alamos, New Mexico 87545, USA*
* *Corresponding authors: lihuang2002@hit.edu.cn; chenht@lanl.gov*

Compiled August 29, 2011

We present the design, numerical simulations and experimental measurements of THz metamaterial absorbers with a broad and flat absorption top both for transverse electric and transverse magnetic polarizations over a wide incidence angle range. The metamaterial absorber unit cell consists of two sets of structures resonating at different but close frequencies. The overall absorption spectrum is the superimposition of individual components and becomes flat at the top over a significant bandwidth. The experimental results are in excellent agreement with numerical simulations.

OCIS codes: 160.3918, 230.3990, 300.6495, 320.7080

Since the first demonstration by Landy et al. [1], metamaterial absorbers have attracted a great deal of interest worldwide during the past few years due to a host of potential applications including detectors, imaging, and sensing. They typically comprise two structured metallic layers separated with a dielectric spacer, either free standing or supported by a suitable substrate, with a total thickness of functional layers much smaller than the operational wavelength. The originally proposed bottom structured metallic layer was a resonant cut-wire array [1,2], which has evolved to a simpler metal ground plane [3]. This makes the metamaterial absorbers more or less resemble Salisbury screens or circuit analog absorbers [4]. A variety of metamaterial structures have been employed and the operational frequency has covered from microwave [1] through terahertz (THz) [2,3,5] to optical [6–8] ranges. The generally accepted idea was that by tuning the effective electric permittivity ϵ and magnetic permeability μ independently, it is possible to realize impedance matching to free-space [1] and minimize the reflection. However, it has been recently found that a Fabry-Perót resonance between the two metallic layers is responsible for the observed metamaterial absorption [9], where the tuned reflection/transmission amplitude and phase by the metamaterial layers satisfy the antireflection requirements similar to a quarter wave antireflection. This is a mechanism that we have verified for many metamaterial absorbers proposed in literature [10].

Besides its polarization and incidence angle dependence, the bandwidth of a metamaterial absorber is one of the important aspects that may affect many applications. So far most designs of metamaterial absorbers operate at a specific narrow frequency range. Dual-band [11–13] and triple-band [14, 15] metamaterial absorbers have been demonstrated with distinct narrow absorption frequencies; however, broadband metamaterial absorbers remain a challenge and there have been only a few very recent studies, mostly focusing on theoretical and numerical investigation [16–20]. In this Letter, we experimentally demonstrate metamaterial absorbers operating in the THz frequency range with a broad and flat high absorption top over a wide incidence angle range, which are in excellent agreement with numerical simulations.

The schematic of THz metamaterial absorber unit cell is shown in Figs. 1(a) and 1(b), which comprises three I-shaped resonators separated from a ground plane using a dielectric spacer. It is symmetrically designed that the two side I-shaped resonators are identical and differ from the center resonator only in the length of the end loading, i.e. $l_1 = 21.5$ μm and $l_2 = 16.5$ or 17.5 μm in our two designs. Finite-element numerical simulations were first performed with CST Microwave Studio 2009 using periodic boundary conditions and under normal incidence, for the electric field parallel to the long axis of the resonators (Fig. 1(a)). The absorptivity $A(\omega)$ was then obtained from the S-parameters by $A(\omega) = 1 - R(\omega) - T(\omega) = 1 - |S_{11}|^2 - |S_{12}|^2$, where $T(\omega)$ is very close to zero when using a gold ground plane of 200 nm thickness, which is the same as in the I-shaped resonators. Three differently configured metamaterial absorbers, as shown in the insets to Fig. 1(c), were simulated using a relative dielectric constant $\epsilon_s = 3.1$ and loss $\tan\delta = 0.07$ for the dielectric spacer (polyimide) of thickness $t = 8.5$ μm. All of them exhibit strong absorption of THz radiation with a peak absorptivity close to unity. The absorption peak is narrow for the configurations with either center (configuration I) or side (configuration II) I-shaped resonators alone. However, deploying the two types of resonators in one unit cell (configuration III) results in a broader absorption top, a superimposition of configurations I and II. Further simulations show that the bandwidth increases as the frequency difference between the absorption peaks of I and II increases; how-

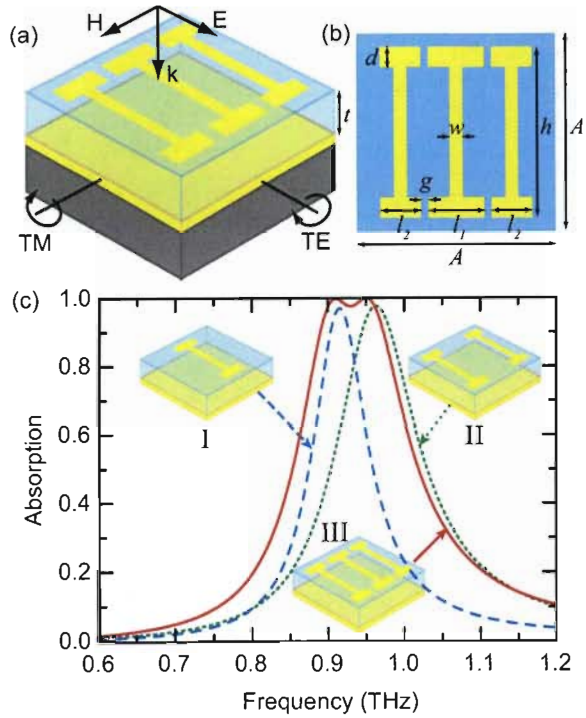

Fig. 1. Schematic of the whole unit cell (a) and top view (b) of the metamaterial absorber with dimensions (in μm) $A = 78$, $h = 68$, $d = 8$, $w = 5$, $t = 8.5$, $g = 2.5$, $l_1 = 21.5$, and $l_2 = 16.5$ or 17.5. TE and TM polarizations are also indicated in (a). (c) Numerical simulation results of absorption spectra at normal incidence for three different configurations of the I-shaped resonators indicated in the insets.

ever, the small dip in III also becomes undesirably wider and deeper. On the other hand, when the absorption peaks of I and II are closer, the absorption top is flatter but with a reduced overall bandwidth.

Two metamaterial absorbers of configuration III were fabricated using parameters shown in the caption of Fig. 1. First, the ground plane was deposited by e-beam evaporation of 10-nm-thick Ti, 200-nm-thick Au, and then again 10-nm-thick Ti on a GaAs substrate. The dielectric spacer was formed using a spin-coated and thermally cured polyimide layer with a final thickness of $\sim$8 μm. Finally, the I-shaped resonator array was patterned using conventional photolithography methods, e-beam deposition of 10-nm-thick Ti and 200-nm-thick Au, and lift-off processes. Note that the purpose of the Ti layers is to increase the adhesion of Au layer to the GaAs substrate and polyimide spacer. The metamaterial absorbers were characterized by reflection measurements using a fiber-coupled THz time-domain spectrometer in reflection mode [9, 21] at various incidence angles between 30° and 60°, using a blank Au coated substrate as the reference.

The absorption spectrum of the metamaterial absorber with $l_2 = 16.5$ μm (sample #1) is shown as the solid curve in Fig. 2, matching well the prediction in Fig. 1. It was measured at an incidence angle of 30° and with the THz electric field parallel to the resonators, i.e. transverse electric (TE) polarization. The measured highest absorptivity is 99.9% at 0.905 and 0.956 THz, between which the smallest absorptivity in the dip is still as high as 93%. The width of the absorption top is 0.1 THz even if we define a strict criterion of 80% of the maximum absorption, and the roll-off is rather fast for broadband operation. As described before, we can largely eliminate the absorption dip by making a smaller frequency difference between the absorption peaks in configurations I and II. This is clearly verified by the dotted absorption spectrum in Fig. 2 obtained from a second metamaterial absorber (sample #2) by slightly increasing $l_2 = 17.5$ μm, which reduces the absorption peak frequency of configuration II, while all other parameters are kept the same as in sample #1. Between 0.899 THz and 0.939 THz (a width of 40 GHz) the absorptivity remains higher than 99%, although the width of the absorption top, as defined above, is slightly reduced to 0.08 THz.

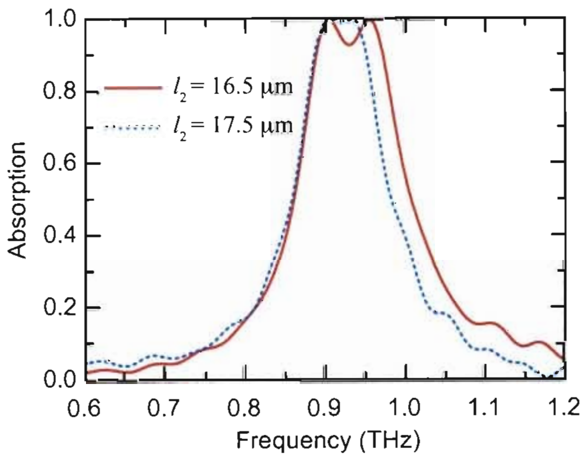

Fig. 2. Measured THz absorption spectra of two metamaterial absorbers with $l_2 = 16.5$ μm (solid red curve) and 17.5 μm (dotted blue curve) for TE polarization and at a 30° incidence angle.

We further characterized the incidence angle dependence of the absorption, which is shown in Fig. 3(a) for sample #1 and TE polarization. Increasing the incident angle results in an overall decrease of the absorptivity and the dip becomes deeper in the absorption spectra. At the large incident angle of 60°, the peak absorptivity is 90% and the smallest absorptivity in the absorption dip is still as high as 74%. The absorption band does not shift with the incidence angle, and the width of the absorption top does not have any significant change. The corresponding numerical simulation results are shown in Fig. 3(b), which are in excellent agreement with experimental measurements. The numerical simulations also reveal that at small incidence angles between 0 and 30° the absorption spectra have very little variation. Additional simulations have been performed with TM polarization as a function of incidence angle, and the meta-

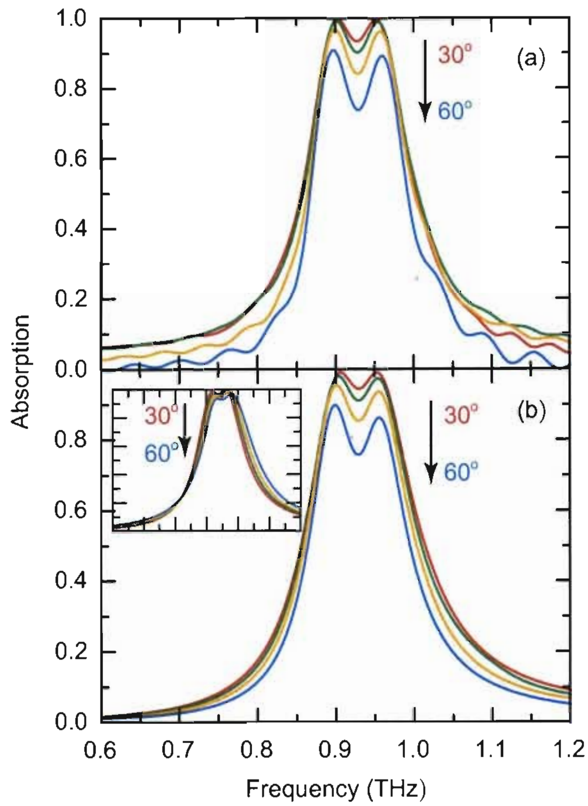

Fig. 3. Measured (a) and simulated (b) absorption spectra for TE polarization at various incidence angles from 30° to 60° with an increment of 10°. Inset: simulated absorption spectra for TM polarization.

material absorption spectra are shown in the inset to Fig. 3. Increasing the incidence angle causes slight shifting, however, the absorptivity and the small absorption dip are almost independent on the incidence angle, a highly desirable property in metamaterial absorbers for many applications.

In summary, we have designed and experimentally demonstrated THz metamaterial absorbers with a broad and flat absorption top over a wide incidence angle range for both TE and TM polarized THz radiation. The experimental results are in excellent agreement with numerical simulations. Further expanding the absorption bandwidth is possible by improving the metamaterial design, and the concept could be readily extended to other frequency regimes for a host of applications that have a wide bandwidth requirement.

L.H. acknowledges support from Natural Science Foundation of China (NSFC) under Grant No. 10904023. We acknowledge support from the Los Alamos National Laboratory LDRD program. This work was performed, in part, at the Center for Integrated Nanotechnologies, a US Department of Energy, Office of Basic Energy Sciences Nanoscale Science Research Center operated jointly by Los Alamos and Sandia National Laboratories. Los Alamos National Laboratory, an affirmative action/equal opportunity employer, is operated by Los Alamos National Security, LLC, for the National Nuclear Security Administration of the US Department of Energy under contract DE-AC52-06NA25396.

References

1. N. I. Landy, S. Sajuyigbe, J. J. Mock, D. R. Smith, and W. J. Padilla, Phys. Rev. Lett. **100**, 207402 (2008).
2. H. Tao, N. I. Landy, C.M. Bingham, X. Zhang, R. D. Averitt, and W. J. Padilla, Opt. Express **16**, 7181 (2008).
3. H. Tao, C. M. Bingham, A. C. Strikwerda, D. Pilon, D. Shrekenhamer, N. I. Landy, K. Fan, X. Zhang, W. J. Padilla, and R. D. Averitt, Phys. Rev. B **78**, 241103 (2008).
4. B. A. Munk, *Frequency Selective Surfaces: Theory and Design* (Wiley, 2000).
5. D. Y. Shchegolkov, A. K. Azad, J. F. OHara, and E. I. Simakov, Phys. Rev. B **82**, 205117 (2010).
6. X. Liu, T. Starr, A. F. Starr, and W. J. Padilla, Phys. Rev. Lett.**104**, 207403 (2010).
7. N. Liu, M. Mesch, T. Weiss, M. Hentschel, and H. Giessen, Nano Lett. **10**, 2342 (2010).
8. K. B. Alici, A. B. Turhan, C. M. Soukoulis, and E. Ozbay, Opt. Express **19**, 14260 (2011).
9. H.-T. Chen, J. F. Zhou, J. F. O'Hara, F. Chen, A. K. Azad, and A. J. Taylor, Phys. Rev. Lett. **105**, 073901 (2010).
10. H.-T. Chen, J. F. OHara, A. K. Azad, and A. J. Taylor, Laser Photonics Rev. **5**, 513 (2011).
11. Q.-Y. Wen, H.-W. Zhang, Y.-S. Xie, Q.-H. Yang, and Y.-L. Liu, Appl. Phys. Lett. **95**, 241111 (2009).
12. H. Tao, C. M. Bingham, D. Pilon, K. Fan, A. C. Strikwerda, D. Shrekenhamer, W. J. Padilla, X. Zhang, and R. D. Averitt, J. Phys. D: Appl. Phys. **43**, 225102 (2010).
13. Y. Ma, Q. Chen, J. Grant, S. C. Saha, A. Khalid, and D. R. S .Cumming, Opt. Lett. **36**, 945 (2011).
14. H. Li, L. H. Yuan, B. Zhou, X. P. Shen, Q. Cheng, and T. J. Cui, J. Appl. Phys. **110**, 014909 (2011).
15. X. Shen, T. J. Cui, J. Zhao, H. F. Ma, W. X. Jiang, and H. Li, Opt. Express **19**, 9401 (2011).
16. C. Hu, L. Liu, Z. Zhao, X. Chen, and X. Luo, Opt. Express **17**, 16745 (2009).
17. Y. Q. Ye, Y. Jin, and S. He, J. Opt. Soc. Am. B **27**, 498 (2010).
18. H. Wakatsuchi, S. Greedy, C. Christopoulos, and J. Paul, Opt. Express **18**, 22187 (2010).
19. H. Luo, Y. Z. Cheng, and R. Z. Gong, Eur. Phys. J. B **81**, 387 (2011).
20. K. B. Alici, A. B. Turhan, C. M. Soukoulis, and E. Ozbay, Opt. Express **19**, 14260 (2011).
21. J. F. O'Hara, E. Smirnova, H.-T. Chen, A. J. Taylor, R. D. Averitt, C. Highstrete, M. Lee, and W. J. Padilla, J. Nanoelectron. Optoelectron. **2**, 90 (2007).